

Climate Change and Agriculture Research Paper

Cite this article: Lai L, Kumar S, Rastogi D, Ashfaq M (2022). Temporal variabilities of soil carbon dioxide fluxes from cornfield impacted by temperature and precipitation changes through high-frequent measurement and DAYCENT modelling. *The Journal of Agricultural Science* **160**, 138–151. <https://doi.org/10.1017/S0021859622000132>

Received: 27 July 2021

Revised: 12 March 2022

Accepted: 20 March 2022

First published online: 31 March 2022

Key words:

Climate change; maize field; model prediction; soil surface CO₂ emission; South Dakota

Author for correspondence:

Liming Lai, E-mail: Liming.lai@qq.com

Temporal variabilities of soil carbon dioxide fluxes from cornfield impacted by temperature and precipitation changes through high-frequent measurement and DAYCENT modelling

Liming Lai^{1,2} , Sandeep Kumar² , Deeksha Rastogi³ and Moetasim Ashfaq³

¹Department of Agronomy, Hetao College, Banyannur, Inner Mongolia, China; ²Department of Agronomy, Horticulture and Plant Sciences, South Dakota State University, Brookings, South Dakota, USA and

³Computational Sciences and Engineering Division, Oak Ridge National Laboratory, Oak Ridge, Tennessee, USA

Abstract

Soil carbon dioxide (CO₂) emissions from the field of corn (*Zea mays* L.) play an important role in global warming. This study investigated temporal variability of soil CO₂ fluxes (R_s) with soil temperature (T_s) and moisture (θ) and built DAYCENT models for predicting future impacts of climate changes on R_s using the measured high-frequency data. R_s trend was tested by Mann–Kendall and Sen Estimator. Predicted R_s s under different climate scenarios were compared using Parallel-line Analysis. The findings indicated that daily R_s exponentially increased with T_s constrained by θ . During the θ of 27–31%, there was a strong exponential relationship between R_s and T_s , but the relationship was weaker for the θ of 38–41% and 22–26%. Soil environmental index (SEI, $T_s \times \theta$) significantly impacted R_s with linear regression $R_s^{0.5} = 0.4599 + 0.002059 \times \text{SEI}$ in 2008, 2009 and 2011. At the diurnal scale, there were different trends in R_s s and relationships among R_s and T_s and θ in different years. Predicted yearly R_s s, root R_s s and corn yield in 2014–2049 increased with an increase in temperature scenarios, but the R_s s significantly increased as temperature rose by 1°C or higher. Predicted yearly R_s s, root R_s s and yield reduced with precipitation scenario increase, and the root R_s s and yield significantly diminished as precipitation increased by 15 and 30%. Predicted yearly R_s from cornfields had a significantly increasing trend. Future research is needed to explore methods for mitigating cornfield R_s and evaluating sensitivities of different cropland R_s s to temperature changes.

Introduction

Carbon dioxide (CO₂) is the principal greenhouse gas (GHG) contributing positively to global warming potential (Reilly *et al.*, 2003). CO₂ emissions from soils have long been identified as the largest natural source of carbon to the atmosphere in most undisturbed and unmanaged terrestrial systems (Diaz-Diaz and Loague, 2001) and as the most significant component of terrestrial ecosystem respiration (Duxbury, 1994; Doherty, 2010). The soil CO₂ emission to the atmosphere is a primary mechanism of carbon (C) loss from soils (Lamers *et al.*, 2007). The emissions come mainly from the decomposition of soil organic matter (SOM) (GGWG, 2010). The main processes of SOM decomposition are biological oxidation by microbes and roots, resulting in soil respiration (Andrews *et al.*, 1999; Lamers *et al.*, 2007; Hernandez-Ramirez *et al.*, 2009). Soil respiration is primarily a combination of two sources: soil autotrophic respiration (mainly from plant roots) and soil heterotrophic respiration (majorly from soil microbes) (Lai *et al.*, 2017; Zheng *et al.*, 2021). The soil CO₂ emission flux (R_s) is controlled by several factors, including soil temperature (T_s), soil moisture (θ) (they strongly depend on air temperature and precipitation), quantity and quality of SOM, soil pore-size distribution, wind speed (Latshaw and Miller, 1924; Linn and Doran, 1984; Raich and Schlesinger, 1992; Lee *et al.*, 2007, 2012), tillage and residue management (Lewandowski *et al.*, 2003; Glenn *et al.*, 2012). The R_s between atmosphere and soil is an essential pathway in the C cycle. The processes that mediate these fluxes can increase the atmospheric concentration of CO₂ (Glenn *et al.*, 2012), causing an increase in global mean surface temperatures (Hofmann *et al.*, 2019).

Corn (*Zea mays* L.) is one of the three major crops [wheat (*Triticum aestivum* L.), corn and rice (*Oryza glaberrima* L. or *Oryza sativa* L.)] in the world. The corn area is 13.69% of the total global cropland area, and the United States of America (USA) is the largest corn producer in the world, with 33 270 820 ha of land reserved for corn production (FAO, 2020). The global and USA corn acreages have been increasing since 1961 (FAO, 2020) due to the corn multi-usage such as food, forage and bioenergy feedstock (Li *et al.*, 2019). Soil management practice is one of the significant factors affecting the soil–atmosphere exchange of GHG

(Watson *et al.*, 1996). Therefore, the CO₂ emissions from soils in the global cornfields play an essential role in global warming.

Previous studies have reported different treatment effects on soil CO₂ emissions from cornfields, such as the tillage effects on CO₂ emissions (Jackson *et al.*, 2001; Johnson and Curtis, 2001; Glenn *et al.*, 2012), the impact of drainage water management on soil CO₂ fluxes (Johnson *et al.*, 2001), the effect of in-field management of corn cob and residue mix on soil CO₂ emissions (Hsu *et al.*, 1985) and CO₂ emissions under different fertilizer treatments (Kanerva *et al.*, 2007). Several studies have reported the temporal variability of R_s at diurnal (Kiniry *et al.*, 1999; Gaumont-Guay *et al.*, 2006; Riveros-Iregui *et al.*, 2007; Kirkham, 2011; Wang *et al.*, 2014) and seasonal time scales (Kiniry *et al.*, 1999; Kutsch *et al.*, 2009; Liu *et al.*, 2009; Kuzyakov and Gavrichkova, 2010; Martin *et al.*, 2012; Wang *et al.*, 2014). However, in the north-central region of the USA, little is known about the daily, seasonal and annual variabilities of R_s from cornfields.

The correlations between R_s and T_s or θ are different depending on various local conditions such as temperature and precipitation. The strong relationship between R_s and T_s was reported by several previous studies (Borken *et al.*, 2006; Arevalo *et al.*, 2010). CO₂ fluxes increase with an increase in temperature, which stimulates microbial activity (Winkler *et al.*, 1996) and enhances root respiration (Rochette and Flanagan, 1997; Arevalo *et al.*, 2010). It is impossible to measure the accurate T_s response of R_s and the confounding effects of T_s with other factors on R_s (Subke and Bahn, 2010). The impacts of θ on R_s are distinct only when the soil is too dry or too wet (Davidson *et al.*, 1998). It is recognized that θ and R_s might have an indirect relationship due to a hysteresis effect in the θ changes on R_s changes (Pacaldo, 2012). Therefore, continuous automated measurements can be beneficial in understanding the relationships between R_s and T_s or θ over time.

The continuous automated soil CO₂ measurement can generate high-frequency temporal data of CO₂ fluxes from the soil. The measured high-frequency R_s is one of the most valuable incomings to calibrate and validate a model that simulates major ecosystem processes. In this study, the DAYCENT model (Parton *et al.*, 1987) was calibrated using the high-frequency R_s data for simulating and predicting R_s from a cornfield. This prediction is vital to make policies or decisions for mitigating GHG emissions. Therefore, the objectives of this study were to (i) explore the temporal variabilities of R_s at seasonal and diurnal time scales from a cornfield located in South Dakota and analyse the relationships among R_s , T_s and θ , (ii) calibrate and validate DAYCENT model, (iii) predict future impacts of climate change scenarios on R_s and corn yield using the built model and (iv) forecast the long-term R_s from cornfield using the built model and the projected climate data by the climate models.

Materials and methods

Data measurements

The study site is near Lennox, South Dakota, USA (43°14'27.0'' N, 96°54'09.0'' W; altitude: 384 m above sea level). Before 1977, the site was an uncultivated field with wild grasses. From 1977 to 2001, the soybean, corn, spring wheat with unregular crop rotations were planted at the site. In 2002–2015, the corn was continuously planted every year at the site, at which the cornfield was not ploughed (i.e. no-tillage; but it was harrowed using the

disc harrows before planting) and applied nitrogen (N) fertilization twice with an N rate of 6.7 (10 days after planting) and 5.6 g N/m² (30–35 days after planting) for each growing season. The R_s from the cornfield were measured using a high frequent measurement method with the Automated Soil CO₂ Flux System, which was LI-8100 instrumentation (LI-COR Biosciences Inc., Lincoln, NE, USA). T_s and θ at the 8-cm depth were also measured using the same LI-8100 equipment (the soil moisture sensors from the LI8100 were previously calibrated). The Automated Soil CO₂ Flux System connected the four gas chambers and sensors to measure R_s , T_s and θ . Two gas chambers and sensors were installed between the cornrows, and the other two were within the rows and were always in the same spot from 2008 to 2011. The four chambers and sensors were located within a 4-meter distance. The hourly R_s , T_s and θ were continually measured in the growing seasons of corn in 2008 and 2009. The 2-h R_s , T_s and θ were continually measured in the 2011 corn growing season. In 2010, most measured values were incorrect because the flooding submerged the four chambers in the field. The formula for the calculation of soil CO₂ flux:

$$R_s = \frac{10VP_0 \left(1 - \frac{W_0}{1000}\right) \partial C'}{RS(T_0 + 273.15) \frac{\partial C'}{\partial t}}$$

where R_s is the soil CO₂ flux (μmol/m²/s), V is volume (cm³), P_0 is the initial pressure (kPa), W_0 is the initial water vapour mole fraction (mmol/mol), R is Gas Constant (8.314 Pa m³/K/mol), S is soil surface area (cm²), T_0 is the initial air temperature (°C) and $\partial C'/\partial t$ is the initial rate of change in water-corrected CO₂ mole fraction (μmol/mol) from time 0 to t . $C'(t)$ v. t data were obtained from a soil CO₂ flux measurement. The data are marked to show when the chamber closed and opened. The details of $C'(t)$ v. t calculation were described in the Using the LI-8100A Soil Gas Flux System and the LI-8150 Multiplexer (LI-8100A manual: <https://licor.app.boxenterprise.net/s/jtpq4vg358reu4c8r4id>).

The means of R_s , T_s and θ measured from the four chambers (i.e. averages of four values were calculated from the four chambers simultaneously) were used to analyse this study. The daily mean R_s (R_{sd}), T_s (T_{sd}) and θ (θ_d) were used to conduct the analyses at the seasonal time scale. The R_{sd} , T_{sd} and θ_d were calculated by averaging the values of R_{sh} , T_{sh} and θ_h during each observed day. The hourly or 2-h R_s (R_{sh}), T_s (T_{sh}) and θ (θ_h) were used for analysis at the diurnal time scale. Yearly (annual) R_s (R_{sy}) was used for showing the modelling results (i.e. predicted results using models).

The daily maximum and minimum air temperature and precipitation data from 1906 to 2013 were retrieved from the nearest Weather Station (14 km) in Centerville, South Dakota. The daily mean air temperature was calculated from the daily maximum and minimum air temperature. The daily mean air temperature in 2008, 2009, 2010 and 2011 were 6.58, 7.16, 8.23 and 8.22 °C, respectively. The annual precipitation in 2008, 2009, 2010 and 2011 were 768, 693, 901 and 562 mm, respectively. The means of air temperature and annual precipitation over the past 30 years (1984–2013) were 8.22 °C and 653 mm. 2011 was a drought year because the precipitation (562 mm) was lower than the long-term annual mean precipitation of 653 mm and the other three observed years. Corn yield was measured from 2008 to 2011. The data for soil bulk density (1.37 Mg/m³), pH (6.7) and particle size distribution (22.5% clay, 37.7% silt and

39.8% sand) were obtained from the USDA-NCSS soil survey (<http://casoilresource.lawr.ucdavis.edu/gmap/>). The field capacity and wilting point were automatically estimated by DAYCENT model software, in which the field capacity was water content at the option of -0.33 bar for the loam soil, and the wilting point was assumed to be water content at -15 bars (Gupta and Larson, 1979; Rawls *et al.*, 1982).

Soil CO₂ flux prediction

DAYCENT model (Stand-alone Version 08/17/2014) was used to simulate and predict R_s in this study. The DAYCENT is the daily version of the CENTURY ecosystem model (Parton *et al.*, 1987), a fully resolved ecosystem model that simulates all major ecosystem processes, such as changes in SOM, plant productivity, nutrient cycling, CO₂ respiration, soil water and soil temperature at the daily scale (Del Grosso *et al.*, 2001). The model inputs included daily precipitation, maximum and minimum daily temperature, soil texture, pH, field capacity, wilting point, historical land use and field and crop management information. The historical land-uses were a series of temperate tall grass and clover grass from year 1 through 1977, soybean (*Glycine max* L.), corn and wheat rotation from 1978 to 2001, and corn from 2002 to 2013. These inputs were used to construct the local DAYCENT model.

However, the performance of this model strongly depends on how well it is calibrated and validated for the specific environmental conditions being evaluated (Smith *et al.*, 1997; De Gryze *et al.*, 2010). The model was calibrated using the Combined Parameter estimation (Doherty, 2010) and Trial-Error (CPTe) methodology, which was described in our previous publications (Mbonimpa *et al.*, 2015; Lai *et al.*, 2016). First, this study used the 'trial and error' method to calibrate the DAYCENT model. Then, the model was calibrated manually by adjusting values of the critical parameters until the adjusted parameters improved the simulations of CO₂ fluxes. However, we could not obtain the best DAYCENT model through manual calibration. Therefore, the PEST model was used to calibrate the manually calibrated DAYCENT model further. First, the 42 most sensitive parameters (Table S1) were selected by running PEST with DAYCENT model from 87 parameters can be adjusted in a total of 599 parameters for simulating crops in the DAYCENT model (Lai *et al.*, 2016). Then, the PEST with DAYCENT models were run for calibration using the 42 most sensitive parameters and the measured CO₂ flux data from the corn growing seasons in 2008 and 2009. The calibrated modelled CO₂ fluxes were extracted from the outputs of the PEST calibrated model, and then the modelled *v.* measured CO₂ fluxes (R_{sd}) were compared. For model evaluation, we used the measured CO₂ flux data from the corn growing seasons in 2011 to validate the DAYCENT model (all the measurements in 2010 were not correct due to flooding). Also, the data of corn yield, T_s and θ were used to validate the model. Based on the DAYCENT model developer, the net primary productivity (NPP) is the most critical parameter for the model validation (if the NPP for the site is incorrect, then none of the other model outputs can be expected to be representative of the conditions at the site). The corn yield can check the NPP for the study site (Parton *et al.*, 1998). Therefore, the corn yield is necessary to validate the calibrated DAYCENT model. The model was validated by comparing the calibrated DAYCENT modelled outputs (i.e. CO₂ flux, corn yield, T_s and θ) to the measured data.

Then, the calibrated and validated DAYCENT model was used to simulate R_s for the long-term (we selected 2014 to 2049) using climate change (i.e. temperature and precipitation changes) scenarios. The temperature scenarios were created based on the incremental scenarios development (McCarthy, 2001). Temperature scenario I (ST1, baseline temperature) in the next 36 years is the past 36-years (from 1978 to 2013) temperature. The climate data over the past 100 years showed no increasing trend in temperature (Fig. S1). Therefore, we developed scenarios II, III and IV (ST2, ST3 and ST4) by increasing the temperature by 0.5, 1.0 and 1.5°C for the next 36 years (from 2014 to 2049), respectively, and keeping the precipitation constant. The five scenarios of precipitation changes (SP1-SP5) from 2014 to 2049 were created based on the changes in precipitation from SP1 to SP5 corresponding to -30 , -15 , 0 , $+15$ and $+30\%$ of the precipitation measured from 1978 to 2013 (SP3 is the precipitation in 1978–2013, i.e. baseline precipitation). The precipitation frequencies for future climate scenarios were kept the same as that of 1978 to 2013. The range was based on that reported by IPCC's projected precipitation to be approximately between -30 to 30% across the globe by 2090 relative to 1990 (IPCC, 2007), and the temperature was kept the same to the increasing trend from 1978 to 2013 (Lai *et al.*, 2016).

The calibrated and validated DAYCENT model was also used for predicting R_s in the next 36 years based on the projected climate data using a nine-member high-resolution regional climate model ensemble. This was generated using the International Centre for Theoretical Physics Regional Climate Model Version 4 (RegCM4, https://www.int-res.com/articles/cr_oa/c052p001.pdf), driven by the 6-hourly initial and boundary forcing from Global Climate Models (GCM) that were part of the 5th phase of the Coupled Model Intercomparison Project (CMIP5). Each RegCM4 integration covered 1965–2005 using the historical simulations and 2010–2050 using the Representative Concentration Pathway 8.5 (RCP 8.5) (Ashfaq *et al.*, 2016). The nine downscaled CMIP5 GCMs include the Beijing Climate Center Climate model (BCC-CSM), Community Climate System Model (CCSM4), Centro Euro-Mediterraneo sui Cambiamenti Climatici Climate Model (CMCC-CM) (Scoccimarro *et al.*, 2011), Flexible Global Ocean-Atmosphere-Land System model (FGOALS) (Oleson *et al.*, 2004), Institute Pierre Simon Laplace Climate Model 5 running on a low-resolution grid (IPSL-CM5A-LR), Model for Interdisciplinary Research on Climate 5 (MIROC5), Max-Planck-Institute Earth System Model running on medium resolution grid (MPI-ESM-MR), Meteorological Research Institute Coupled ocean-atmosphere General Circulation Model (MRI-CGCM3) (Yukimoto *et al.*, 2012), and the Norwegian Earth System Model (NorESM1-M) (Bentsen *et al.*, 2013). RegCM4 simulations were conducted at 18 km horizontal grid spacing with 18-levels in the vertical over a domain covering the continental United States and parts of Canada and Mexico (Ashfaq *et al.*, 2016). The output from the RegCM4 simulations was further bias-corrected to 4 km using the methodology detailed in Ashfaq *et al.* (2013). Finally, the bias-corrected data was used to extract the simulated temperature for the 10 points representing the study site.

Statistical analysis

The trend analysis for the measured data was conducted by using the Mann-Kendall test (the null hypothesis states that there is no monotonic trend) (Mann, 1945; Kendall, 1975; Gilbert, 1987) with slopes estimated by the Sen estimator (Sen, 1968) using

the package ‘*mblm*’ in R (Komsta, 2013; R Core Team, 2020). The data autocorrelation coefficients were calculated, and Autocorrelation Function (ACF) plots were drawn using the R language (R Core Team, 2020). The line plots, scatter plots with trend lines and their functions, and tables were made using Microsoft Excel 2019. Parallel-line analysis was used for comparing the simulated R_s s under different climate scenarios using SAS 9.4 (SAS, 2013). The parallel-line analysis is a statistical method for comparing two datasets that are time-correlated or paired values that are not independent. It can determine whether linear regression slopes and intercepts of the two datasets are significantly different. If the slopes are not significantly different (i.e. the two-line slopes are parallel), it can test whether the line intercepts are significantly different. If the slopes are significantly different, there is no sense in testing line intercepts (Solusions4u, 2021). The distributions of the datasets were tested for normality using the Kolmogorov-Smirnov method using SAS 9.4 (SAS, 2013) when exploring the datasets. Data were transformed when necessary for building a regression model. The transformation was determined using the Box-Cox method (Box and Cox, 1964, 1982) using SAS 9.4 (SAS, 2013). Pearson correlation coefficient (r) was calculated using SAS 9.4 (SAS, 2013). Significance was determined at $\alpha = 0.05$ level for all statistical analyses.

Performance of the calibrated and validated DAYCENT model was evaluated with four widely used quantitative criteria (Moriyas *et al.*, 2007; Dai *et al.*, 2014) that include the determination coefficient (R^2 , squared correlation coefficient), per cent bias (PBIAS) (Gupta *et al.*, 1999), model performance efficiency (ME/NSE) (Nash and Sutcliffe, 1970) and the root mean squared error (the RMSE) and RSR (the ratio of RMSE to SD (standard deviation of measured data)) (Singh *et al.*, 2004). The acceptable range of the four evaluation criteria R^2 , PBIAS, ME/NSE and RSR are 0.5 to 1, –25 to 25%, 0.5 to 1 and 0 to 0.7, respectively (Table S2).

Results

Soil hourly CO_2 fluxes and corn yield

Soil hourly (2008 and 2009) and 2-h (2011) CO_2 fluxes ($n = 38\,416$) are the original measured data, presented in Fig. 1 and Fig. S2. Data showed that, in general, the hourly and 2-h R_s displayed a seasonal trend with the temperature change, such as higher R_s from mid-June to mid-August and lower R_s in other periods for each year (Fig. 1). The maximum and minimum values of the hourly and 2-h R_s were 11.8575 and $-0.1225 \mu\text{mol}/\text{m}^2/\text{s}$ (there was a total of 2 negative values). The median, mean and standard deviation of hourly and 2-h R_s were 2.4120, 2.8250 and 1.9355 $\mu\text{mol}/\text{m}^2/\text{s}$, respectively. The values of hourly and 2-h R_s did not follow a normal distribution. The hourly and 2-h R_s values between 0 and 3 $\mu\text{mol}/\text{m}^2/\text{s}$ had a higher frequency, and the values greater than 8 $\mu\text{mol}/\text{m}^2/\text{s}$ had a smaller frequency (Fig. S2). Several hourly and 2-h R_s values increased or decreased suddenly, and a few values were extraordinarily high and low (Fig. 1(a)).

The corn yield at this study site was 10 432, 11 700, 9949 and 9591 kg/ha in 2008, 2009, 2010 and 2011, respectively.

Seasonal soil daily CO_2 fluxes and soil temperature and moisture

The daily CO_2 fluxes (R_{sd}) and daily soil temperature (T_{sd}) and moisture (θ_d) at the seasonal time scale are presented in Figs 2

to 4, Figs. S3 to S10 and Table 1. In 2008, the median, mean and standard deviation of R_{sd} were 2.7, 3.3 and 2.3 $\mu\text{mol}/\text{m}^2/\text{s}$, respectively. The maximum and minimum values of R_{sd} were 8.3 and 0.30 $\mu\text{mol}/\text{m}^2/\text{s}$, respectively. R_{sd} had an increasing trend from 13 June to 30 July 2008, and a decreasing trend from 30 July to 18 November 2008, with fluctuations (Fig. 2(a)). T_{sd} followed a decreasing trend in the 2008 growing season (Fig. 2(b)). However, θ_d showed a flat pattern throughout the growing season with large fluctuations (Fig. 2(c)). Further, the trend tests showed that, overall, R_{sd} and T_{sd} followed a significantly reducing trend over time (P value < 0.0001 with negative slopes). In contrast, θ_d did not follow a significant trend (P value = 0.71). The first-order and second-order autocorrelation coefficients (r_1 and r_2) for R_{sd} , T_{sd} and θ_d were greater than 0.65, which indicated that these three variables had time-series autocorrelation. Further, the r_1 and r_2 for R_{sd} and T_{sd} were greater than that for θ_d (Table 1). The ACF plots further displayed that the R_{sd} , T_{sd} and θ_d exhibited autocorrelation with their 14, 14 and 6 lags (days), respectively (Fig. S5). There was an exponential relationship with high R^2 between R_{sd} and T_{sd} in the corn production field for the growing season in 2008: $R_{sd} = 0.2826e^{0.12827T_{sd}}$ ($R^2 = 0.90$) (Fig. 3(a)). However, corresponding to different θ_d , the exponential relationships were different. The three ranges of soil moisture were decided by splitting the θ_d dataset in 2008 into three groups with the same amount of data, namely, 22–26%, 27–31% and 32–37%. During the range of 32–37% of θ_d , there was a strong exponential relationship with high R^2 (0.9) between R_{sd} and T_{sd} , and the exponential relationship was very strong ($R^2 = 0.95$) for the 27–31% of θ_d . However, for the low θ_d condition (soil moisture of 22–26%), the exponential relationship was weak (close linear relationship) (Fig. S8). There was a fairly weak relationship between R_{sd} and θ_d in 2008 (Fig. 4). However, the relationship between CO_2 and the product of T_s and θ ($T_s \times \theta$), which is called the soil environment index (SEI), was strong. The outputs of the linear regression model ($R_{sd}^{0.5} = b + a \times SEI + \varepsilon$, $R_{sd}^{0.5}$ is 0.5 power of R_{sd}) in 2008 showed that a (coefficient of SEI in the model) was positive and P value < 0.0001 (Table 2), indicating that the SEI had a significant positive impact on the R_{sd} in the cornfield. R^2 was 0.77 (Table 2), indicating the 77% of the variance in the $R_{sd}^{0.5}$ that the SEI could explain.

In 2009, the median, mean and standard deviation of R_{sd} were 2.3, 2.4 and 1.4 $\mu\text{mol}/\text{m}^2/\text{s}$, respectively, and the maximum and minimum values of R_{sd} were 5.1039 and 0.1580 $\mu\text{mol}/\text{m}^2/\text{s}$, respectively. R_{sd} followed a decreasing trend from 17 May to 7 June and 26 June to 30 October 2009, and an increasing trend from 7 June to 26 June 2009, with fluctuations (Fig. S3(a)). T_{sd} followed a decreasing trend in 2009, and θ_d did not show an obvious trend (Fig. S3(b) and (c)). Further, the trend analysis showed that R_{sd} and T_{sd} followed an overall decreasing trend over time (P value < 0.0001 with negative slopes). In contrast, θ_d did not follow a significant trend (P value = 0.42) (Table 1). The first-order and second-order autocorrelation coefficients (r_1 and r_2) for R_{sd} , T_{sd} and θ_d were > 0.45 , which indicated that these three variables had time-series autocorrelation. Further, r_1 and r_2 values for R_{sd} and T_{sd} were greater than those for θ_d (Table 1). The ACF plots further showed that R_{sd} , T_{sd} and θ_d had autocorrelation with 12, 12 and 3 lags (days), respectively (Fig. S6). There was an exponential relationship between R_{sd} and T_{sd} for the corn growing season in 2009: $R_{sd} = 0.1586e^{0.14527T_{sd}}$ ($R^2 = 0.86$) (Fig. 3(b)). During the range of 32–37% of θ_d , there was a strong exponential relationship with high R^2 (0.90) between R_{sd} and T_{sd} , and for the 27–31% of θ_d , the exponential relationship was still strong

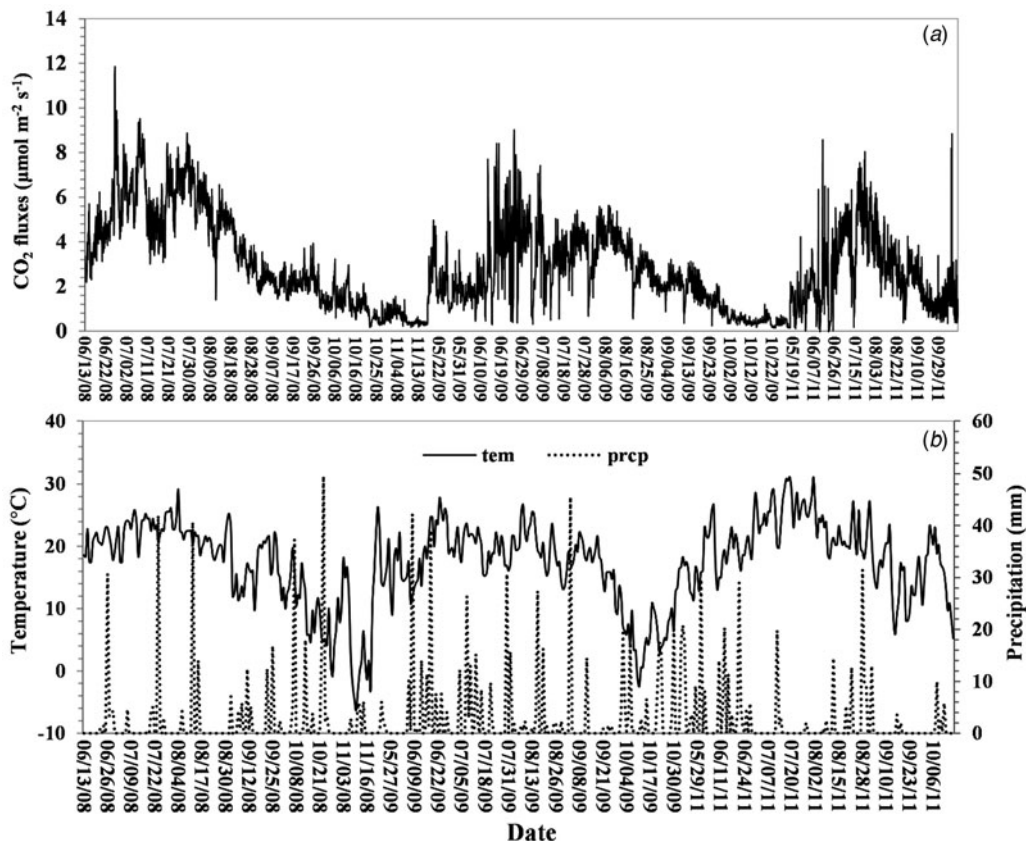


Fig. 1. (a) Soil hourly (2008 and 2009) and 2-hour (2011) CO₂ fluxes (μmol/m²/s) and (b) daily air temperature (tem) and precipitation (prcp) data corresponding to the measured days in 2008, 2009 and 2011 from the cornfield at the South Dakota site.

($R^2 = 0.82$) (Fig. S9). However, there were only five values of R_{sd} under the low θ_d condition (22–26%), which were too small to reveal a correct relationship. There was a fairly weak relationship between R_{sd} and θ_d in 2009 (Fig. 4). The linear regression model ($R_{sd}^{0.5} = b + a \times SEI + \varepsilon$) in 2009 showed that the a was positive and P value < 0.0001 (Table 2), indicating that the SEI had a significant positive impact on the R_{sd} in the cornfield. R^2 was 0.72 (Table 2), indicating the 72% of the variance in the $R_{sd}^{0.5}$ that the SEI could explain.

In 2011, the median, mean and standard deviation values of R_{sd} were 2.4, 2.6 and 1.4 μmol/m²/s, respectively, with the maximum and minimum values of 6.6 and 0.18 μmol/m²/s, respectively (Fig. S4(a)). R_{sd} had an increasing trend from 17 May to 18 July, 2011, and a decreased trend from 18 July to 16 October 2011 (Fig. S4(a)). T_{sd} showed the same trend in R_s (Fig. S4(b)). θ_d followed a decreasing trend (Fig. S4(c)). Further, the trend tests showed that R_{sd} , T_{sd} and θ_d followed a significantly decreased trend over the observed days (P value = 0.024, < 0.0001 and < 0.0001 with negative slopes, respectively). The first-order and second-order autocorrelation coefficients (r_1 and r_2) of R_{sd} , T_{sd} and θ_d were greater than 0.78, which indicated the three variables had time-series autocorrelation. The r_1 and r_2 of T_{sd} and θ_d were greater than that of R_{sd} (Table 1). The ACF plots further showed that, overall, R_{sd} , T_{sd} and θ_d had autocorrelation with their 10, 12 and 12 lags (days), respectively (Fig. S7). There was an exponential relationship between R_{sd} and T_{sd} in 2011: $R_{sd} = 0.3098e^{0.10287T_{sd}}$ ($R^2 = 0.53$) (Fig. 3(c)). Specifically, for the high θ_d (38–41%), there was no obvious relationship between R_{sd} and T_{sd} . For the ranges of 32–37%, 27–31% and 22–26% of θ_d ,

there were exponential relationships between R_{sd} and T_{sd} with 0.43, 0.74 and 0.57 of R^2 , respectively (Fig. S10). There were strong relationships (a curve) between R_{sd} and θ_d in 2011, in which the R_{sd} was highest when the soil moisture was 30.80%. When the $\theta_d < 30.80\%$, the R_{sd} increased as the θ_d increased. When the $\theta_d > 30.80\%$, the R_{sd} reduced as the θ_d increased (Fig. 4). The linear regression model ($R_{sd}^{0.5} = b + a \times SEI + \varepsilon$) in 2011 showed that the a was positive and P value < 0.0001 (Table 2), indicating that the SEI had a significant positive impact on the R_{sd} in the cornfield. R^2 was 0.28 (Table 2), indicating the 28% of the variance in the $R_{sd}^{0.5}$ that the SEI could explain.

Diurnal soil CO₂ fluxes and soil temperature and moisture

R_{sh} , T_{sh} and θ_h at the diurnal time scale are presented in Figs 5 and 6 and Figs. S11 to S13. In 2008, R_{sh} , T_{sh} and θ_h had a similar pattern. There was a linear relationship between R_{sh} and T_{sh} : $R_{sh} = 0.029T_{sh} + 2.8756$ ($R^2 = 0.52$). Also, the linear relation between R_{sh} and θ_h was: $R_{sh} = 0.3436\theta_h - 6.6463$ ($R^2 = 0.48$). The relationship between R_{sh} and T_{sh} did not display daily hysteresis (Figs. 5 and S11(d)). The diurnal patterns of R_{sh} , T_{sh} and θ_h with standard deviation in 2008 are shown in Fig. S11.

In 2009, R_{sh} , T_{sh} and θ_h followed a similar pattern. There was a linear relationship between R_{sh} and T_{sh} : $R_{sh} = 0.1719T_{sh} - 0.6452$ ($R^2 = 0.81$). The linear relationship between R_{sh} and θ_h was: $R_{sh} = 1.0201\theta_h - 30.442$ ($R^2 = 0.85$) (Fig. 6). The relationship between R_{sh} and T_{sh} displayed a daily hysteresis loop (Fig. 6(a)).

In 2011, R_{sh} and θ_h had a similar pattern. However, T_{sh} had different from the pattern of R_{sh} and θ_h . There was a linear

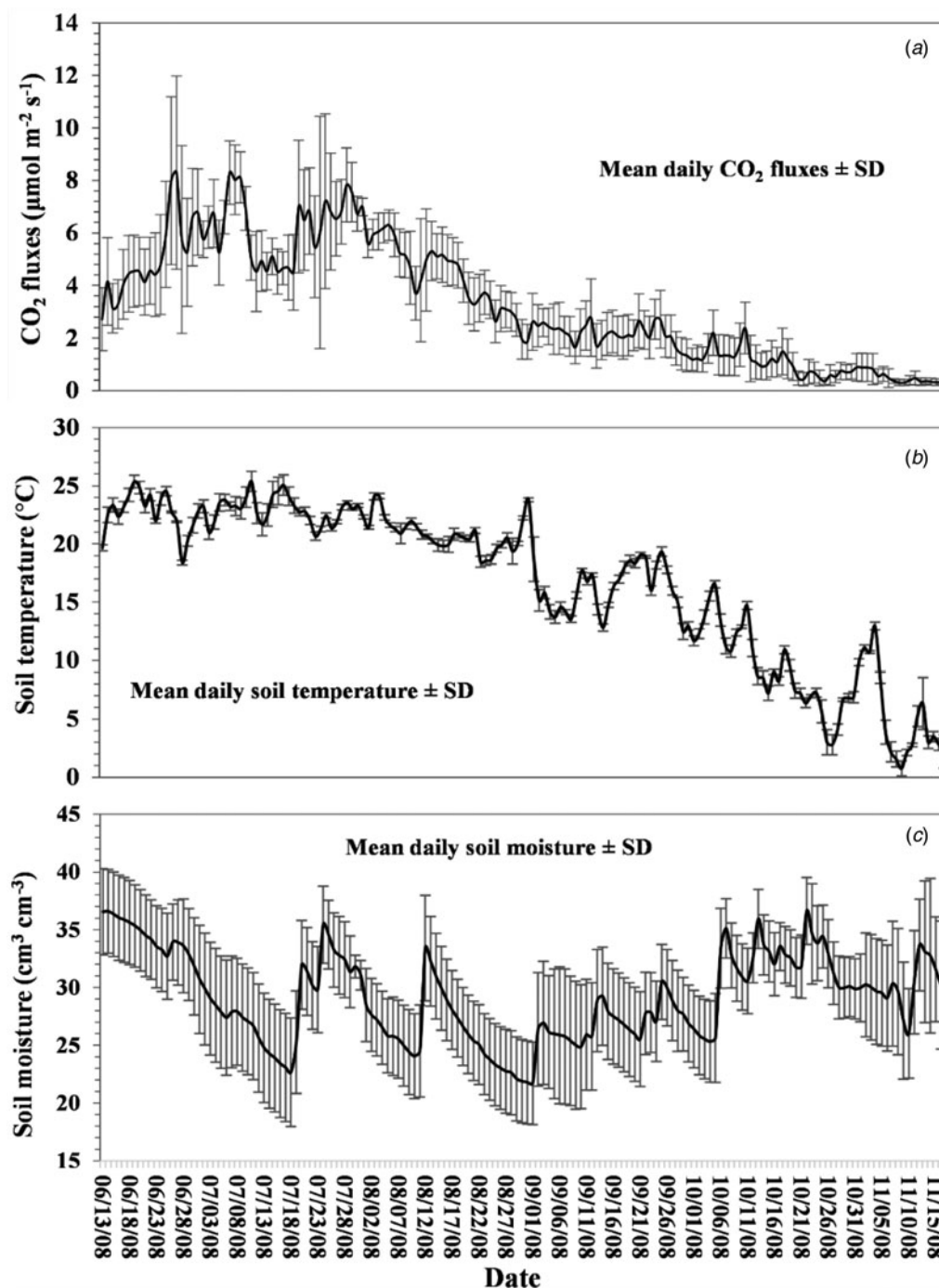


Fig. 2. (a) Means of daily soil CO₂ flux (R_{sd}) \pm s.d. (standard deviation of values of four chambers), (b) means of daily soil temperature (T_{sd}) \pm s.d. (standard deviation of values of four chambers) and (c) means of daily soil moisture (θ_d) \pm s.d. (standard deviation of values of four chambers) from the cornfield at the South Dakota site in 2008.

relationship between R_{sh} and T_{sh} : $R_{sh} = 0.0071T_{sh} + 2.5056$ with $R^2 = 0.0036$. The linear relationship between R_{sh} and θ_h was: $R_{sh} = 1.3289\theta_h - 37.884$ with $R^2 = 0.66$. The relationship of R_{sh} and T_{sh} displayed a daily hysteresis loop (Fig. S13(d)).

Calibration and validation of DAYCENT model

The calibrated results using the measured R_s showed that the values of determination coefficient (R^2), PBIAS, modelling

efficiency (ME/NSE) and RSR (ratio of RMSE to SD of measured R_s) were 0.71, 1.4%, 0.71 and 0.54, respectively, which were within the acceptable ranges of the four evaluation criteria (Table S2). The simulated and measured R_s in the calibration period had a similar trend and magnitude with few unaligned peaks (Fig. S14). Based on the validated results, for T_s , the values of R^2 , PBIAS, ME and RSR were 0.80, 1.10%, 0.71 and 0.54, respectively, which were acceptable. The corresponding values for θ were 0.51, -2.7%, 0.02 and 0.99, respectively, in which the R^2 and

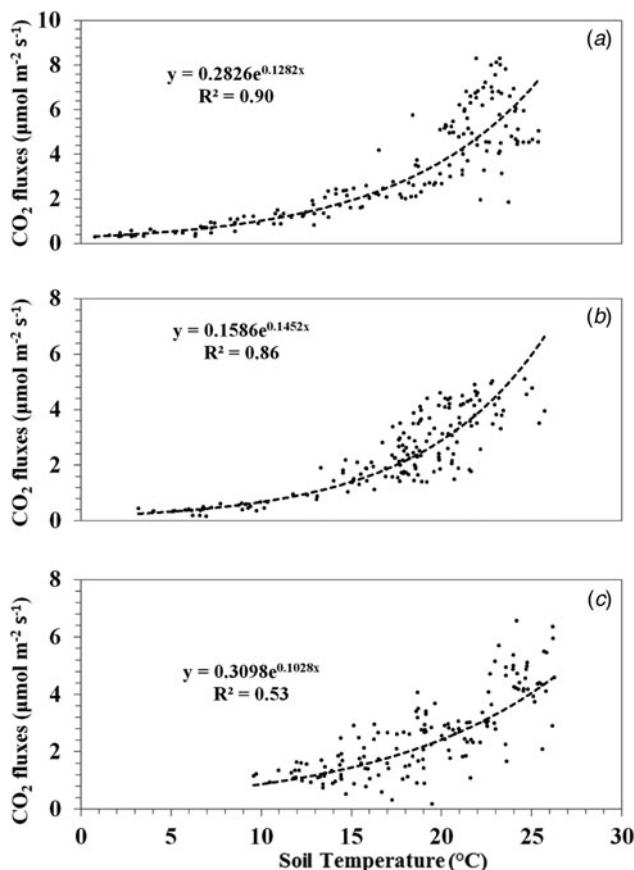


Fig. 3. The exponential relationship between daily soil CO₂ fluxes (R_{sd}) and daily soil temperature (T_{sd}) measured in the cornfield at the South Dakota site in (a) 2008, (b) 2009 and (c) 2011. y = daily soil CO₂ flux (R_{sd}); x = daily soil temperature (T_{sd}); R^2 = determination coefficient.

PBIAS were acceptable but ME and RSR were out of the acceptable ranges. However, the R^2 (0.84) and PBIAS (1.10%) values for corn yield were acceptable (Table S2). Therefore, generally, this study's calibrated and validated DAYCENT model was acceptable.

Modelling future impacts of temperature and precipitation changes on annual soil CO₂ fluxes, root CO₂ fluxes and corn yield

In response to four temperature scenarios, ST1, ST2, ST3 and ST4, the four simulated annual soil CO₂ fluxes RT1, RT2, RT3 and RT4 for the next 36 years (2014–2049) are presented in Table 3. For the soil CO₂ fluxes, the RT1 (ST1: baseline temperature) and RT4 (ST4: +1.5°C) were significantly different (P value = 0.018). The RT3 (ST3: +1.0°C) and RT1 were marginally different ($0.05 \leq P$ value < 0.10). RT2 *v.* RT1, RT4 *v.* RT2, RT3 *v.* RT2 and RT4 *v.* RT3 were not significantly different (P value > 0.11). The means of RT1, RT2, RT3 and RT4 had an increasing trend with increasing temperature scenarios (Table 3). For the root CO₂ fluxes, the RT1–4 were not significantly different from one another, and the means of RT1–4 increased as the temperature scenarios increased (Table 3). The corn yields in response to four temperature scenarios were not significantly different from one another (Table 3).

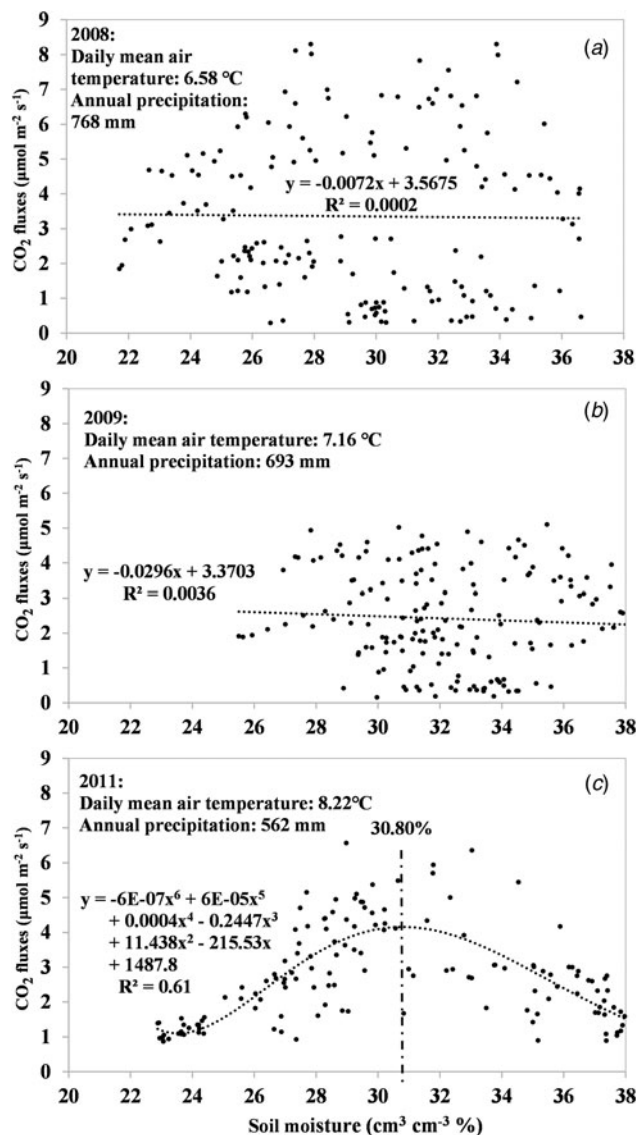


Fig. 4. Relationships between daily soil CO₂ fluxes (R_{sd}) and daily soil moisture (θ_{sd}) measured in the cornfield at the South Dakota site in (a) 2008, (b) 2009 and (c) 2011. y = daily soil CO₂ flux (R_{sd}); x = daily soil moisture (θ_{sd}); R^2 = determination coefficient.

In response to five precipitation scenarios SP1–5 (–30%, –15%, +0, +15%, +30% Precipitation from 1978 to 2013, which is baseline precipitation, i.e. SP3), the five simulated annual soil CO₂ fluxes RP1–5 for the next 36 years (2014–2049) are presented in Table 4. For the soil CO₂ fluxes, the RP4 and RP2 were marginally significantly different ($0.05 \leq P$ value < 0.10). The RP2 *v.* RP3, RP4 *v.* RP3, RP5 *v.* RP3, RP1 *v.* RP2 and RP5 *v.* RP4 were not significantly different. The RP1 *v.* RP3, RP5 *v.* RP2, RP4 *v.* RP1 and RP5 *v.* RP1 were unable to be compared because the line slopes are significantly different based on the parallel line analysis. For the root CO₂ fluxes, the RP5 was significantly lower than the RP3. The RP4 *v.* RP3, RP4 *v.* RP2 and RP5 *v.* RP2 were marginally different. Other paired RPs were not significantly different. The means of RP1–5 reduced as the precipitation scenarios increased (Table 4). The corn yield under the SP5 was significantly lower than that for the SP3 and SP2. The corn yield under the SP4 was marginally lower than that for the SP3 and SP2. Other paired yields were not significantly different (Table 4).

Table 1. The *P* values of Mann–Kendall test for analysing the trend over time (days), slopes using Sen Estimator and first-order and second-order autocorrelation coefficients (r_1 and r_2)

	R_{sd}^a	T_{sd}	θ_d
2008			
<i>P</i> value	<0.0001	<0.0001	0.71
Slope	−0.04048	−0.1225	0.000141
r_1	0.955	0.955	0.838
r_2	0.914	0.908	0.656
2009			
<i>P</i> value	<0.0001	<0.0001	0.42
Slope	−0.02989	−0.05441	−0.00475
r_1	0.897	0.945	0.734
r_2	0.809	0.894	0.453
2011			
<i>P</i> value	0.024	<0.0001	<0.0001
Slope	−0.02093	−0.0809	−0.10979
r_1	0.887	0.931	0.956
r_2	0.786	0.84	0.906

^a R_{sd} is the daily soil CO₂ fluxes (μmol/m²/s); T_{sd} is the daily mean soil temperature (°C); θ_d is the daily mean soil moisture (%; cm³/cm³).

Predicted future long-term soil CO₂ fluxes

Comparisons of all pairs of ten projected soil CO₂ fluxes corresponding to ten projected weather data showed that within a total of 45 pairs of the predicted CO₂ fluxes, 12 pairs were significantly different (*P* value < 0.05), and the other 33 pairs were not significantly different (*P* values > 0.05) (Table S4). The 12 significant different pairs likely implied that the projected weather data corresponding to the 12 pairs had significant differences. However, most pairs of soil CO₂ fluxes (73.3%) were not significant. Therefore, generally, the projected weather data were acceptable.

Means and 95% confidence intervals of predicted R_{sy} for the next 36 years are presented in Fig. 7 and Table S3. The means had an increasing trend over the years: $R_{sy} = 3.0548 \times \text{year} + 609.33$ ($R^2 = 0.80$) (Fig. 7). The trend test showed that the slope was 3.1578 with a very small *P* value (<0.0001). Based on the equation, the predicted mean of R_{sy} in 2014 and 2049 were 612.38 and 719.30 g/m²/year, respectively, which had a difference of 106.92 g/m²/year. The mean of predicted R_{sy} in 2015 was 611.49 g/m²/year, and its 95% confidence interval was [569.33, 653.64] (Table S3). The mean predicted R_{sy} from 2014 to 2049 was 665.85 g/m²/year. The mean 95% confidence intervals of predicted R_{sy} for the means of predicted R_{sy} in the next 36 years were 628.48 to 703.22 g/m²/year.

Discussion

Seasonal variabilities of soil CO₂ fluxes influenced by soil temperature and moisture and their interaction in the cornfield

The findings from this study showed that the seasonal variabilities of R_{sd} were closely linked to T_{sd} and θ_d . The R_{sd} increased

exponentially with T_{sd} (Fig. 3). There was a robust exponential relationship between R_{sd} and T_{sd} during the 27–31% range of θ_d . However, there were relatively weak relationships between R_{sd} and T_{sd} for the ranges of 38–41% or 22–26% of θ_d (Figs. S8–S10). Previous studies have reported the exponential dependence of respiration rate on temperature. It was originated by Van't Hoff in 1898 (Lloyd and Taylor, 1994). Lloyd and Taylor (1994) used natural logarithms to express the case of respiration rate. Furthermore, Kominami *et al.* (2012) confirmed the exponential relationship and presented their function in 2012: $R_s = 0.0566e^{0.0717T_s} \left(\frac{\theta}{\theta+0.1089} \right)$ which was at a depth of 5-cm in their study site located in a mountainous region of western Japan. In this study, the exponential relationships of R_s with T_s were changed in different ranges of θ . This is likely related to the confounding effect of the association between T_s and θ .

The SEI influences R_s in most ecosystems (Li *et al.*, 2006; Kanerva *et al.*, 2007), but the relationships between R_s and SEI in the ecosystems are different. A study reported that the SEI was linearly related to R_s (Amacher and Mackowiak, 2011). However, they only had a single year of temporal variation in R_s . In this study, we have the 3-year data, and there was a power relationship between R_s and SEI, namely, $R_s = i + k \times \text{SEI}^2$ or $R_s^{0.5} = b + a \times \text{SEI}$. However, the degrees of relationships in 2008, 2009 and 2011 differed (Table 2 and Fig. S15). For example, the SEI can explain 77, 72, 28 and 51% of the variance in the $R_s^{0.5}$ in 2008, 2009, 2011 and the three years, respectively (Table 2). As the SEI increased by one unit, the $R_s^{0.5}$ increased 0.28, 0.24, 0.13 and 0.21% in 2008, 2009, 2011 and the three years, respectively (Table 2). The SEI can impact R_s likely because the precipitation can impact soil respiration by altering both soil temperature and moisture (Gabriel and Kellman, 2014; Deng *et al.*, 2018), and the temperature can influence soil CO₂ by changing the soil temperature and soil moisture by evapotranspiration (Poll *et al.*, 2013), but deeper reasons should be further investigated.

Furthermore, the scatter plots of R_s and SEI showed that R_s gradually changed (i.e. increased or reduced) as SEI increased (Fig. S15). This is because as the SEI increased, the $T_s \times \theta$ mainly resulted in three possible situations: high T_s and low θ , moderate T_s and θ and/or low T_s and high θ . (i) When T_s was high and θ was low, the SOM decomposition and root respiration are slow due to depression of low θ (Jensen *et al.*, 2003; Smith *et al.*, 2003; Mbonimpa *et al.*, 2015), resulting in lower R_s . (ii) T_s and θ were moderate, leading to the SOM fast decomposed, mainly resulting in higher R_s (Raich and Schlesinger, 1992; Schimel and Clein, 1996; Giorgi *et al.*, 1998). (iii) When low T_s and high θ occurred, the SOM slowly decomposed owing to the low T_s that reduces soil biological activity (Al-Kaisi and Yin, 2005), specifically, high θ in soils reduced transpiration due to increased stomatal resistance or anaerobic conditions by flood, thereby reducing or blocking CO₂ emissions from soils (Liu *et al.*, 2002; Kirkham, 2011).

Diurnal variabilities of soil CO₂ fluxes from cornfield impacted by soil temperature and moisture

The findings in this study showed distinct diurnal patterns of R_{sh} in 2008, 2009 and 2011. The relationships among R_{sh} , T_{sh} and θ_h at a diurnal time scale in 2008, 2009 and 2011 differed. No lags were found in 2008, but daily hysteresis loops in 2009 and 2011 were displayed (Figs. 6(a) and S13(d)). The lags between R_{sh} and T_{sh} have also been observed in other ecosystems and vary

Table 2. Outputs of linear regression model ($\text{CO}_2^{0.5} = b + a \times \text{SEI} + \varepsilon$) in 2008, 2009, 2011 and the 3 years

Regression outputs ^a	2008	2009	2011	3 years
R^2	0.77	0.72	0.28	0.51
P values for testing model	<0.0001	<0.0001	<0.0001	<0.0001
b	0.3328	0.1809	0.7504	0.4599
a	0.002829	0.002362	0.00134	0.002059
P values for testing a	<0.0001	<0.0001	<0.0001	<0.0001

SEI, soil temperature (T_s) \times soil moisture (θ); ε , model residues
^a R^2 , determination coefficient; a , coefficient of SEI in the model. b , intercept in the model.

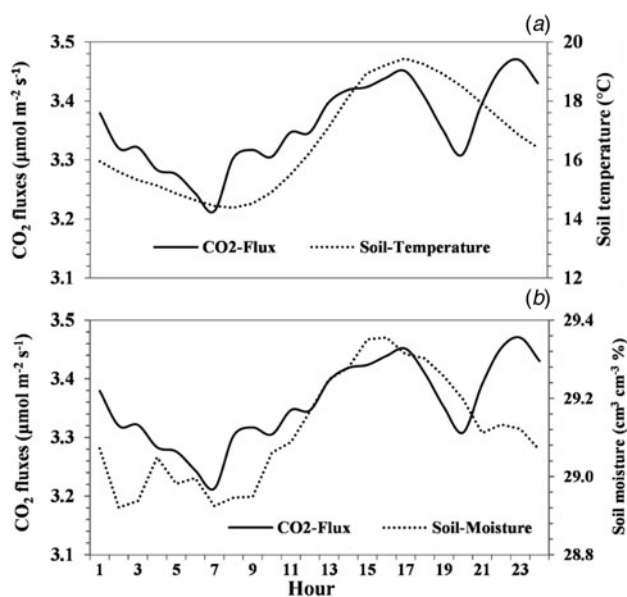


Fig. 5. Diurnal pattern of hourly CO_2 fluxes (R_{sh}) and (a) hourly soil temperature (T_{sh}) and (b) hourly soil moisture (θ_h) from the cornfield at the South Dakota site in 2008.

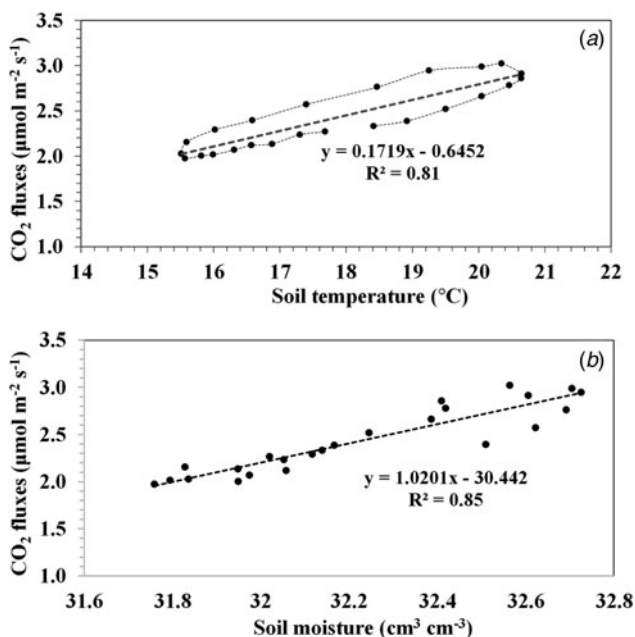


Fig. 6. (a) Diurnal hourly CO_2 fluxes R_{sh} v. hourly soil temperature T_{sh} and (b) R_{sh} v. hourly soil moisture θ_h in 2009. y = hourly soil CO_2 flux (R_{sh}); (A) x = hourly soil temperature (T_{sh}) and (B) x = hourly soil moisture (θ_h); R^2 = determination coefficient.

Table 3. Means and P values of comparisons of the predicted annual soil CO_2 fluxes, root autotrophic CO_2 fluxes (R_{sy} ; RT1, RT2, RT3 and RT4) and corn yield in response to four scenarios of temperature (ST1, ST2, ST3 and ST4)

Temperature scenarios ^a	Soil CO_2 (R_{sy})	Root CO_2 (R_{sy})	Corn yield
	P values ^b		
ST4_v_ST1	0.02	0.61	0.76
ST3_v_ST1	0.092	0.33	0.53
ST2_v_ST1	0.41	0.17	0.38
ST4_v_ST2	0.11	0.64	0.74
ST3_v_ST2	0.38	0.40	0.56
ST4_v_ST3	0.47	0.71	0.81
	Annual mean (s.d.) ($\text{g}/\text{m}^2/\text{year}$)		Yield (s.d.) (kg/ha)
ST1	604.0 (51.2)	170.2 (26.0)	10 508 (1214.3)
ST2	613.2 (53.4)	173.2 (25.5)	10 597 (1129.2)
ST3	623.0 (55.2)	175.9 (24.1)	10 688 (1051.1)
ST4	631.1 (56.8)	177.9 (22.6)	10 753 (978.70)

^aST1 is the temperature scenario 1 from 2014 to 2049, which is the past 36-year temperature and precipitation from 1978 to 2013 at this study site. S2, S3 and S4 are temperature scenario 2, 3 and 4, respectively, which are an increase of temperature by 0.5, 1 and 1.5 °C in the next 36 years from 2014 to 2049, respectively, and keeping the precipitation constant, which was same as the precipitation from 1978 to 2013.

^b P values were from the results using the Parallel-line statistical analysis method for comparing the two datasets over time.

seasonally with θ_h (Verstraete and Focht, 1977; Gaumont-Guay *et al.*, 2006; Riveros-Iregui *et al.*, 2007; Kirkham, 2011; Wang *et al.*, 2014). The lags may be caused by a mismatch between the depths of T_s measurement and CO_2 production or by a diurnal variation in the photosynthetic carbon supply which affected the rhizospheric respiration (Kiniry *et al.*, 1999; Li, 2000; Subke and Bahn, 2010). The lags may also be attributed to different autotrophic and heterotrophic respiration responses to environmental factors (Riveros-Iregui *et al.*, 2007). Autotrophic respiration responds to photosynthetically active radiation (Li *et al.*, 2006) and air temperature, whereas heterotrophic respiration responds primarily to T_s (Lloyd and Taylor, 1994; Winkler *et al.*, 1996). Maybe plant photosynthesis is a factor in influencing diel hysteresis between R_s and T_s (Tang *et al.*, 2005). In this study, the mean θ was 29.17% during the corn growing season in 2008, which was smaller than that in 2009 (32.19%) and 2011 (30.97%). The soil in 2008 was relatively drier. Therefore, the diffusion coefficient of CO_2 in the air-filled pore space was large enough to facilitate the transport of autotrophic and heterotrophic CO_2

Table 4. Means and comparisons of the predicted annual soil CO₂ fluxes, root autotrophic CO₂ (R_{sy} : RP1, RP2, RP3, RP4 and RP5) and corn yield in response to five scenarios of precipitation (SP1, SP2, SP3, SP4 and SP5)

Precipitation scenarios ^a	Soil CO ₂ (R_{sy})	Root CO ₂ (R_{sy})	Corn yield
	<i>P</i> values ^b		
SP1_v._SP3	–	0.862	0.919
SP2_v._SP3	0.468	0.372	0.353
SP4_v._SP3	0.249	0.068	0.076
SP5_v._SP3	0.133	0.041	0.040
SP1_v._SP2	0.975	0.474	0.340
SP4_v._SP2	0.077	0.099	0.054
SP5_v._SP2	–	0.061	0.025
SP4_v._SP1	–	0.35	0.313
SP5_v._SP1	–	0.237	0.175
SP5_v._SP4	0.702	0.779	0.705
	Annual mean (s.d.) (g/m ² /year)		Yield (s.d.) (kg/ha)
SP1	639.3 (88.2)	182.3 (24.5)	10 954 (1344.7)
SP2	639.8 (68.7)	181.4 (23.2)	10 962 (1027.0)
SP3	631.1 (55.5)	177.6 (23.0)	10 753 (993.60)
SP4	619.2 (48.2)	172.7 (22.6)	10 524 (1024.3)
SP5	615.4 (45.5)	171.2 (23.7)	10 429 (1076.8)

^aSP1 is the precipitation scenario 1 from 2014 to 2049, which is the past 36-year temperature and precipitation from 1978 to 2013 at this study site. SP2, SP3, SP4, SP5 are precipitation scenarios 2, 3, 4 and 5, respectively, which are 70%, 85%, 100%, 115% and 130% precipitation in the next 36 years from 2014 to 2049, respectively, and keeping the temperature constant, which was expected to increase by the same trend from 1978 to 2013.

^b*P* values were from the results using the Parallel-line statistical analysis method for comparing the two datasets over time. '–' indicates no *P* value here because the *P* value of interaction between R_{sy} level and years < 0.05 based on the Parallel-line statistical analysis method; this situation (two lines are not parallel) needs to be future analysed for comparing the CO₂ fluxes under different SPs based on different periods from 2014 to 2019.

from the soil. As the soil becomes drier, microbial activity declines and the time lag between photosynthetically active radiation and T_s decreases due to accelerated soil heat diffusion (LI-COR, 2010). This could result in no daily hysteresis loop in 2008. Whereas, in 2009 and 2011, because the θ was higher than that in 2008, the hysteresis was formed between R_{sh} and T_{sh} . (Riveros-Iregui *et al.*, 2007; Liebigh *et al.*, 2008).

In this study, the diel variation of R_s was constrained by θ , which is similar to the results of Wang *et al.* (2014). In contrast, Tang *et al.* reported for an oak-grass savanna that T_s largely controlled the diel variation in R_s , whereas θ did not affect the diel R_s cycle (Tang *et al.*, 2005). Another situation is that the diel variation of θ was negligible or constant over a day while R_s had an obvious diel variation (Gaumont-Guay *et al.*, 2006). In this study, the R_{sh} and θ_h had a relatively strong relationship ($R^2 = 0.48, 0.85$ and 0.66 in 2008, 2009 and 2011, respectively), and there was no apparent daily hysteresis loop between R_{sh} and θ_h . Perhaps, it is attributed to the humid continental climate at this study site. This climate is appropriate for corn to grow well and has a high diurnal temperature range. The high daily temperature range potentially leads to conditions where the soil temperature is lower than the dew-point temperature on most nights. As a result, condensation water often occurs on the ground (Agam and

Berliner, 2006), increasing root activity and inducing a high root respiration rate (Wang *et al.*, 2014).

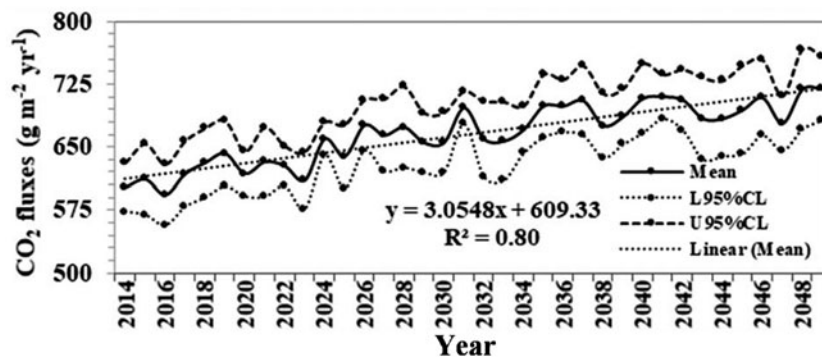
Furthermore, in this study, there was a weak relationship between the diel variation of R_{sh} and T_{sh} ($R^2 = 0.0036$) in 2011. The diel variation of R_{sh} reduced as T_{sh} increased during 14–24 h of the day and T_{sh} decreased during 1–14 h of the day (Fig. S13 (a) and (b)). The specific reasons for this behaviour need to be further explored. However, we speculated that the unusual rainfall in 2011 (the less manual rainfall and several heavy rainfalls in this year) likely diluted or constrained the relationship between R_{sh} and θ_h measured from July to October in 2011.

Predicted soil CO₂ fluxes from cornfields impacted by climate changes

The predicted results in this study using the DAYCENT model showed that the mean annual CO₂ fluxes under the temperature scenarios ST4 and ST3 (i.e. air temperature increase of 1.5 and 1°C) would be 4.49 and 3.15% higher than ST1 in the next 36 years. The impacts of ST4 and ST3 on R_{sy} were significant (Table 3). These findings differ from the results from the switchgrass land in South Dakota, which showed that the impacts of temperature increases of 1°C or higher on R_s were not significant (Lai *et al.*, 2016). Some studies have demonstrated that soil temperature, which is strongly related to air temperature, was the primary factor regulating CO₂ emission in the growing season (Kirschbaum, 1995; Omonode *et al.*, 2007). The significant impacts of ST4 and ST3 on R_{sy} from the cornfield in this study are likely attributed to higher SOM and more appropriate soil microenvironment built by corn plants than that for the switchgrass land, which was a marginal land (Lai *et al.*, 2018), resulting in higher residue decomposition and root respiration in corn than switchgrass (Omonode *et al.*, 2007), subsequently, R_{sy} from cornfield was stronger to soil temperature than for switchgrass. Moreover, the directions of the two effects were similar, as there was an increasing trend over the years. However, the magnitudes of the two effects could not be clearly concluded from the comparisons of predicted soil CO₂ fluxes given that there were several distinct influencing factors, such as different data of soil properties, landscape positions, climate, fertilizers, land-use history and so forth at the two study sites.

The soil R_{sy} s under SP1 (–30%SP3) and SP3 (baseline precipitation) were unable to be compared (Table 4) because the two slope lines were not parallel based on the Parallel-line analysis, indicating that there was a complicated situation impacted under the drought SP1. The soil R_{sy} s under the SP2 (–15% SP3), SP4 (+15%SP3) and SP5 (+30%SP3) were not significantly different than that for the SP3 (Table 4). This is in accord with a previous study that reported that the CO₂ release by aerobic respiration was primarily temperature-dependent but became moisture-dependent as soil dries (Smith *et al.*, 2003). However, the specific impacts of precipitation on GHG emissions from the soil surface are uncertain (Omonode *et al.*, 2007). This is because the soil moisture's strong dependence on precipitation affects soil CO₂ fluxes by directly influencing corn root and microbial activities and indirectly on soil physical and chemical properties (Raich and Schlesinger, 1992; Schimel and Clein, 1996). Moreover, there was a wide range of fluctuations in R_{sy} s under drought conditions (Lai *et al.*, 2016). Therefore, it could not directly compare the R_{sy} s under SP1 (–30%SP3) and baseline precipitation (SP3).

Fig. 7. The means and their 95% confidence interval of forecasting annual soil CO₂ fluxes R_{sy} from the cornfield in South Dakota for the next 36 years using the DAYCENT model based on weather data predicted by ten climate models. y =yearly soil CO₂ flux (R_{sy}); x =year; R^2 =determination coefficient; L95% CL = lower 95% confidence interval; U95% CL = upper 95% confidence interval.



Furthermore, the root R_{sy} under drought SP1 and SP2 were not significantly different from that for the SP3, whereas the root R_{sy} s under wet SP5 and SP4 were significantly lower than that for the SP3 (Table 4). The effect of drought on root R_{sy} depends on the function of plants and the response of plant roots to drought (Zhang *et al.*, 2014). Drought conditions may limit plant growth and decrease the input from litter and the supply of photosynthetic products to the root system and root respiration (Gomez-Casanovas *et al.*, 2012). Drought stress may limit the number and size of soil microbial populations (Manzoni *et al.*, 2012; Zhang *et al.*, 2014). Therefore, the effect of drought on root R_{sy} could be an indirect reflection (Scott-Denton *et al.*, 2006; Zhou *et al.*, 2007; Zheng *et al.*, 2021). The indirect impact may result in an insignificant change in the root R_{sy} under drought conditions. In contrast, excessive precipitation can reduce gaseous connectivity among micropores within soils, temporally reducing oxygen diffusion into and through soils and air-filled porosity (Sextstone *et al.*, 1985), increasing stomatal resistance, hence decreasing CO₂ respiration (Kirkham, 2011) and corn yield, likely resulting in a significantly low root R_{sy} and corn yield (Table 4).

However, statistically testing modelled data can always result from significant differences if simulating for enough years. Therefore, we used the DAYCENT model to predict the 36-year CO₂ flux data at different scenarios in this study. The comparisons for the modelled data were to find significant differences in CO₂ fluxes among different scenarios within the 36 years. The significant differences are relative, not absolute comparisons as with measured data. Therefore, our results from the comparisons were relative among the scenarios within the 36 years, hence reasonable.

Also, the predicted R_{sy} had a significantly increasing trend over the next 36 years in terms of the projected temperature and precipitation from 2014 to 2049 at the South Dakota site using the nine climate models (Fig. 7; the positive slope with P value < 0.0001 based on the trend test). The projected daily mean temperature from 2014 to 2049 had an increasing trend (Fig. S17). The soil CO₂ fluxes exponentially increased with the temperature in the cornfield (Fig. 3). Therefore, there could be a significantly increasing trend in the future soil CO₂ fluxes over time. The mean R_{sy} from 2014 to 2049 was 665.84 g/m²/year, which was 22.3% higher than the mean R_{sy} (544 g/m²/year) from croplands (Raich and Schlesinger, 1992). These results indicated that the soil CO₂ fluxes from cornfields would be significantly higher than the mean R_s from other croplands. Other studies also reported that perennial crops emit less CO₂ emissions than corn (Adler *et al.*, 2007; Lai *et al.*, 2016).

Limitations and further work

The model in this study was calibrated using the CPTE methodology (Mbonimpa *et al.*, 2015; Lai *et al.*, 2016), which can obtain the best model based on the four quantitative criteria (Moriassi *et al.*, 2007; Dai *et al.*, 2014) and improve efficiency and accuracy of model calibration manually using ‘*trial and error*’ method. The measured R_{sd} in 2008, 2009 and 2011 calibrated the DAYCENT model. Of 461 values of measured R_{sd} in the growing seasons in 2008, 2009, 2011 and 19 values had sudden and unexplainable changes and were unable to be captured by the DAYCENT model. Also, the 19 values changed the trend of whole data over time, even though the 19 values are only 4.1% of total observations. To simulate the trend of 95.9% values using the DAYCENT model, the 19 values as outliers were removed.

Some parameters differed by 1 order of magnitude from the default in this study. The default values were determined by the model developer in Colorado, USA, while the model calibration for this study was based on the data collected in South Dakota, USA. The two states have different environmental conditions, soil types, landscapes and other relevant characteristics. The model developer has defined the lower and upper bound for each parameter. All calibrated parameters were in the predefined lower and upper bounds range. This clarifies the need for significant differences from default values for some parameters.

This study reported the temporal variability of soil CO₂ fluxes from a cornfield but no spatial distribution results. This was primarily because the measurement of R_s from multiple sites using the Automated Soil CO₂ Flux System can be costly. However, the soil CO₂ flux spatial distribution is essential for policymakers and producers to find the differences in soil CO₂ emissions at different sites under various climate conditions. Based on the differences in soil CO₂ emissions, one can suggest which regions should grow more corn to mitigate soil CO₂ emissions. Moreover, as stated previously, the R_s from cornfield would be significantly higher than the mean R_s from other croplands. Therefore, future research is needed to (i) use the static chamber method (Hutchinson and Mosier, 1981; Parkin and Venterea, 2010) or flux tower measurement to measure R_s at various sites for evaluating the spatial distribution of R_s in cornfields, (ii) explore different methods such as tillage, fertilization and irrigation methods for mitigating R_s from cornfields and (iii) assessing sensitivities of R_s s from different croplands to changes in temperature to regulate land-use policies.

Conclusions

This study showed the findings of continuous hourly soil CO₂ flux measurements from a cornfield at the South Dakota site, and

especially the temporal variability of measured and modelling soil CO₂ fluxes related to T_s , θ and climate changes. The findings indicate that the daily R_s exponentially increased with T_s constrained by θ . The SEI significantly impacted R_s , but the impacts could be positive or negative based on different quantities of T_s and θ . At the diurnal scale, there were different trends in R_s and dissimilar relationships among R_s and T_s and θ in 2008, 2009 and 2011. The predicted yearly R_s in 2014–2049 significantly increased as the temperature rose by 1°C or higher, but predicted root R_s s and corn yield under different temperature scenarios were not different. The predicted yearly R_s s, root R_s s and corn yield decreased with an increase in precipitation scenarios, but the root R_s s and corn yield significantly reduced as the precipitation increased by 15% or higher. The predicted yearly R_s from the cornfield based on the projected temperature and precipitation using the nine regional climate models had a significantly increasing trend, indicating that the cornfield will generate more soil CO₂ emissions in the future. Future research is needed to evaluate the spatial distribution of R_s , explore different methods to mitigate R_s from cornfields and assess sensitivities of R_s s from different croplands to temperature changes for adjusting land-use policies.

Supplementary material. The supplementary material for this article can be found at <https://doi.org/10.1017/S0021859622000132>

Author contributions. L. L. and S. K. conceptualized and designed the study. D. R. and M. A. projected future climate data. L. L. calibrated and validated the DAYCENT model, predicted CO₂ data, performed statistical analyses, and prepared the manuscript draft. S. K., D. R. and M. A. reviewed and revised the manuscript.

Financial support. The research was supported by the funding provided by the Agricultural Experiment Station of the South Dakota State University. The regional model experiments were conducted using resources of the Oak Ridge Leadership Computing Facility, which is a DOE Office of Science User Facility supported under Contract DE-AC05-00OR22725. M. A. was supported by the National Climate-Computing Research Center, which is located within the National Center for Computational Sciences at the ORNL and supported under a Strategic Partnership Project, 2316-T849-08, between DOE and NOAA.

Conflict of interest. The authors declare there are no conflicts of interest.

Ethical standards. Not applicable.

References

- Adler PR, Grosso SJD and Parton WJ (2007) Life-cycle assessment of net greenhouse-gas flux for bioenergy cropping systems. *Ecological Applications* **17**, 675–691.
- Agam N and Berliner P (2006) Dew formation and water vapor adsorption in semi-arid environments – a review. *Journal of Arid Environments* **65**, 572–590.
- Al-Kaisi MM and Yin X (2005) Tillage and crop residue effects on soil carbon and carbon dioxide emission in corn–soybean rotations. *Journal of Environmental Quality* **34**, 437–445.
- Amacher M and Mackowiak C (2011) Seasonal soil CO₂ flux under big sagebrush (*Artemisia tridentata* Nutt.). *Natural Resources and Environmental Issues* **17**, Article 27. Available at <http://digitalcommons.usu.edu/nrei/vol17/iss1/27> (Accessed 12 October 2017).
- Andrews JA, Harrison KG, Matamala R and Schlesinger WH (1999) Separation of root respiration from total soil respiration using carbon-13 labeling during free-air carbon dioxide enrichment (FACE). *Soil Science Society of America Journal* **63**, 1429–1435.
- Arevalo C, Bhatti JS, Chang SX, Jassal RS and Sidders D (2010) Soil respiration in four different land use systems in North Central Alberta, Canada. *Journal of Geophysical Research: Biogeosciences (2005–2012)* **115**, G01003.
- Ashfaq M, Ghosh S, Kao SC, Bowling LC, Mote P, Touma D, Rauscher SA and Diffenbaugh NS (2013) Near-term acceleration of hydroclimatic change in the western US. *Journal of Geophysical Research: Atmospheres* **118**, 10676–610693.
- Ashfaq M, Rastogi D, Mei R, Kao SC, Gangrade S, Naz BS and Touma D (2016) High-resolution ensemble projections of near-term regional climate over the continental United States. *Journal of Geophysical Research Atmospheres* **121**, 9943–9963.
- Bentsen M, Bethke I, Debernard J, Iversen T, Kirkevåg A, Seland Ø, Drange H, Roelandt C, Seierstad I and Hoose C (2013) The Norwegian earth system model, NorESM1-M-part 1: description and basic evaluation of the physical climate. *Geoscientific Model Development* **6**, 687–720.
- Borken W, Savage K, Davidson EA and Trumbore SE (2006) Effects of experimental drought on soil respiration and radiocarbon efflux from a temperate forest soil. *Global Change Biology* **12**, 177–193.
- Box GEP and Cox DR (1964) An analysis of transformations. *Journal of the Royal Statistical Society. Series B (Methodological)* **26**, 211–252.
- Box GEP and Cox DR (1982) An analysis of transformations revisited, rebutted. *Journal of the American Statistical Association* **77**, 209–210.
- Dai Z, Birdsey RA, Johnson KD, Dupuy JM, Hernandez-Stefanoni JL and Richardson K (2014) Modeling carbon stocks in a secondary tropical dry forest in the Yucatan Peninsula, Mexico. *Water, Air, & Soil Pollution* **225**, 1–15.
- Davidson E, Belk E and Boone RD (1998) Soil water content and temperature as independent or confounded factors controlling soil respiration in a temperate mixed hardwood forest. *Global Change Biology* **4**, 217–227.
- De Gryze S, Wolf A, Kaffka SR, Mitchell J, Rolston DE, Temple SR, Lee J and Six J (2010) Simulating greenhouse gas budgets of four California cropping systems under conventional and alternative management. *Ecological Applications* **20**, 1805–1819.
- Del Grosso S, Parton W, Mosier A, Hartman M, Brenner J, Ojima D and Schimel D (2001) Simulated interaction of carbon dynamics and nitrogen trace gas fluxes using the DAYCENT model. In Shaffer MJ, Ma L and Hansen S (eds), *Modeling Carbon and Nitrogen Dynamics for Soil Management*. Florida, USA: CRC Press, pp. 303–332.
- Deng Q, Zhang D, Han X, Chu G, Zhang Q and Hui D (2018) Changing rainfall frequency rather than drought rapidly alters annual soil respiration in a tropical forest. *Soil Biology and Biochemistry* **121**, 8–15.
- Diaz-Diaz R and Loague K (2001) Assessing the potential for pesticide leaching for the pine forest areas of Tenerife. *Environmental Toxicology and Chemistry* **20**, 1958–1967.
- Doherty J (2010) *PEST, Model-Independent Parameter Estimation – User Manual*. Brisbane, Australia: Watermark Numerical Computing.
- Duxbury JM (1994) The significance of agricultural sources of greenhouse gases. *Fertilizer Research* **38**, 151–163.
- FAO (2020) FAOSTAT crop data – global area harvested, yield, production quantity in 2018. Food and Agriculture Organization (FAO) of the United Nations – Statistics Division (EES). Available at <http://www.fao.org/faostat/en/#data/QC> (Accessed 12 September 2020).
- Gabriel CE and Kellman L (2014) Investigating the role of moisture as an environmental constraint in the decomposition of shallow and deep mineral soil organic matter of a temperate coniferous soil. *Soil Biology & Biochemistry* **68**, 373–384.
- Gaumont-Guay D, Black TA, Griffis TJ, Barr AG, Jassal RS and Nesic Z (2006) Interpreting the dependence of soil respiration on soil temperature and water content in a boreal aspen stand. *Agricultural and Forest Meteorology* **140**, 220–235.
- GGWG (2010) *Agriculture's Role in Greenhouse Gas Emissions and Capture*. Madison, WI: Greenhouse Gas Working Group (GGWP) Rep. ASA, CSSA, and SSSA. Available at <https://www.soils.org/files/science-policy/ghg-report-august-2010.pdf> (Accessed 2 September 2016).
- Gilbert RO (1987) *Statistical Methods for Environmental Pollution Monitoring*. New York, USA: Van Nostrand Reinhold Company Inc.
- Giorgi F, Mearns LO, Shields C and McDaniel L (1998) Regional nested model simulations of present day and 2× CO₂ climate over the central plains of the US. *Climatic Change* **40**, 457–493.
- Glenn AJ, Tenuta M, Amiro BD, Maas SE and Wagner-Riddle C (2012) Nitrous oxide emissions from an annual crop rotation on poorly drained

- soil on the Canadian Prairies. *Agricultural and Forest Meteorology* **166**, 41–49.
- Gomez-Casanovas N, Matamala R, Cook DR and Gonzalez-Meler MA** (2012) Net ecosystem exchange modifies the relationship between the autotrophic and heterotrophic components of soil respiration with abiotic factors in prairie grasslands. *Global Change Biology* **18**, 2532–2545.
- Gupta SC and Larson WE** (1979) Estimating soil water retention characteristics from particle size distribution, organic matter percent, and bulk density. *Water Resources Research* **15**, 1633–1635.
- Gupta HV, Sorooshian S and Yapo PO** (1999) Status of automatic calibration for hydrologic models: comparison with multilevel expert calibration. *Journal of Hydrologic Engineering* **4**, 135–143.
- Hernandez-Ramirez G, Brouder SM, Smith DR and Scoyoc GV** (2009) Greenhouse gas fluxes in an eastern corn belt soil: weather, nitrogen source, and rotation. *Journal of Environmental Quality* **38**, 841–854.
- Hofmann M, Mathesius S, Krieglner E, van Vuuren D and Schellnhuber H** (2019) Strong time dependence of ocean acidification mitigation by atmospheric carbon dioxide removal. *Nature Communications* **10**, 1–10.
- Hsu F, Nelson C and Matches A** (1985) Temperature effects on germination of perennial warm-season forage grasses. *Crop Science* **25**, 215–220.
- Hutchinson GL and Mosier AR** (1981) Improved soil cover method for field measurements of nitrous oxide fluxes. *Soil Science Society of America Journal* **45**, 311–316.
- IPCC** (2007) Climate change 2007: the physical science basis. In Solomon S, Qin D, Manning M, Chen Z, Marquis M, Averyt KB, Tignor M and Miller HL (Eds), *Contribution of Working Group I to the Fourth Assessment Report of the Intergovernmental Panel on Climate Change*. Cambridge, UK: Cambridge University Press, p. 996.
- Jackson RB, Carpenter SR, Dahm CN, McKnight DM, Naiman RJ, Postel SL and Running SW** (2001) Water in a changing world. *Ecological Applications* **11**, 1027–1045.
- Jensen KD, Beier C, Michelsen A and Emmett BA** (2003) Effects of experimental drought on microbial processes in two temperate heathlands at contrasting water conditions. *Applied Soil Ecology* **24**, 165–176.
- Johnson DW and Curtis PS** (2001) Effects of forest management on soil C and N storage: meta analysis. *Forest Ecology and Management* **140**, 227–238.
- Johnson DW, Hungate BA, Dijkstra P, Hymus G and Drake B** (2001) Effects of elevated carbon dioxide on soils in a Florida scrub oak ecosystem. *Journal of Environmental Quality* **30**, 501–507.
- Kanerva T, Regina K, Rämö K, Ojanperä K and Manninen S** (2007) Fluxes of N₂O, CH₄ and CO₂ in a meadow ecosystem exposed to elevated ozone and carbon dioxide for three years. *Environmental Pollution* **145**, 818–828.
- Kendall MG** (1975) *Rank Correlation Methods*, 4th Edn, London, UK: Charles Griffin.
- Kiniry J, Tischler C and Van Esbroeck G** (1999) Radiation use efficiency and leaf CO₂ exchange for diverse C₄ grasses. *Biomass and Bioenergy* **17**, 95–112.
- Kirkham MB** (2011) *Elevated Carbon Dioxide: Impacts on Soil and Plant Water Relations*. London, UK: CRC Press.
- Kirschbaum MUF** (1995) The temperature dependence of soil organic matter decomposition and the effect of global warming on soil organic matter storage. *Soil Biology and Biochemistry* **27**, 753–760.
- Kominami Y, Jomura M, Ataka M, Tamai K, Miyama T, Dannoura M, Makita N and Yoshimura K** (2012) Heterotrophic respiration causes seasonal hysteresis in soil respiration in a warm-temperate forest. *Journal of Forest Research* **17**, 296–304.
- Komsta L** (2013) mblm: median-based linear models. R package version 0.12. Available at <http://CRAN.R-project.org/package=mblm>.
- Kutsch WL, Bahn M and A H** (2009) *Soil Carbon Dynamics: An Integrated Methodology*. New York, USA: Cambridge University Press.
- Kuzyakov Y and Gavrichkova O** (2010) REVIEW: time lag between photosynthesis and carbon dioxide efflux from soil: a review of mechanisms and controls. *Global Change Biology* **16**, 3386–3406.
- Lai L, Kumar S, Chintala R, Owens VN, Clay D, Schumacher J, Nizami A-S, Lee SS and Rafique R** (2016) Modeling the impacts of temperature and precipitation changes on soil CO₂ fluxes from a switchgrass stand recently converted from cropland. *Journal of Environmental Sciences* **43**, 15–25.
- Lai L, Kumar S, Folle SM and Owens VN** (2017) Predicting soils and environmental impacts associated with switchgrass for bioenergy production: a DAYCENT modeling approach. *GCB Bioenergy* **10**, 287–302.
- Lai L, Kumar S, Osborne S and Owens VN** (2018) Switchgrass impact on selected soil parameters, including soil organic carbon, within six years of establishment. *Catena* **163**, 288–296.
- Lamers M, Ingwersen J and Streck T** (2007) Modeling N₂O emission from a forest upland soil: automatic calibration of Forest-DNDC model. *Ecological Modeling* **205**, 52–58.
- Latshaw W and Miller E** (1924) Elemental composition of the corn plant. *Journal of Agricultural Research* **27**, 845–861.
- Lee D, Doolittle J and Owens V** (2007) Soil carbon dioxide fluxes in established switchgrass land managed for biomass production. *Soil Biology and Biochemistry* **39**, 178–186.
- Lee J, Pedroso G, Linquist BA, Putnam D, Kessel C and Six J** (2012) Simulating switchgrass biomass production across ecoregions using the DAYCENT model. *GCB Bioenergy* **4**, 521–533.
- Lewandowski I, Scurlock JM, Lindvall E and Christou M** (2003) The development and current status of perennial rhizomatous grasses as energy crops in the US and Europe. *Biomass and Bioenergy* **25**, 335–361.
- LI-COR** (2010) *LI-8100A Automated Soil CO₂ Flux System & LI-150 Multiplexer Instruction Manual*. Lincoln, NE, USA: LI-COR, Inc.
- Li CS** (2000) Modeling trace gas emission from agricultural ecosystems. *Nutrient Cycling in Agroecosystems* **58**, 259–276.
- Li Y, Xu M and Zou X** (2006) Heterotrophic soil respiration in relation to environmental factors and microbial biomass in two wet tropical forests. *Plant and Soil* **281**, 193–201.
- Li Y, Miao R and Khanna M** (2019) Effects of ethanol plant proximity and crop prices on land-use change in the United States. *American Journal of Agricultural Economics* **101**, 467–491.
- Liebig MA, Schmer MR, Vogel KP and Mitchell RB** (2008) Soil carbon storage by switchgrass grown for bioenergy. *Bioenergy Research* **1**, 215–222.
- Linn D and Doran J** (1984) Effect of water-filled pore space on carbon dioxide and nitrous oxide production in tilled and nontilled soils. *Soil Science Society of America Journal* **48**, 1267–1272.
- Liu X, Wan S, Su B, Hui D and Luo Y** (2002) Response of soil CO₂ efflux to water manipulation in a tallgrass prairie ecosystem. *Plant and Soil* **240**, 213–223.
- Liu W, Zhang Z and Wan S** (2009) Predominant role of water in regulating soil and microbial respiration and their responses to climate change in a semiarid grassland. *Global Change Biology* **15**, 184–195.
- Lloyd J and Taylor J** (1994) On the temperature dependence of soil respiration. *Functional Ecology* **8**, 315–323.
- Mann HB** (1945) Non-parametric tests against trend. *Econometrica* **13**, 163–171.
- Manzoni S, Schimel JP and Porporato A** (2012) Responses of soil microbial communities to water stress: results from a meta-analysis. *Ecology* **93**, 930–938.
- Martin JG, Phillips CL, Schmidt A, Irvine J and Law BE** (2012) High-frequency analysis of the complex linkage between soil CO₂ fluxes, photosynthesis and environmental variables. *Tree Physiology* **32**, 49–64.
- Mbonimpa EG, Gautam S, Lai L, Kumar S, Bonta J, Wang X and Rafique R** (2015) Combined PEST and trial-error approach to improve APEX calibration. *Computers and Electronics in Agriculture* **114**, 296–303.
- McCarthy JJ** (2001) *Climate Change 2001: Impacts, Adaptation, and Vulnerability: Contribution of Working Group II to the Third Assessment Report of the Intergovernmental Panel on Climate Change*. Cambridge, UK and New York, USA: Cambridge University Press.
- Moriassi D, Arnold J, Van Liew M, Bingner R, Harmel R and Veith T** (2007) Model evaluation guidelines for systematic quantification of accuracy in watershed simulations. *Transactions of the ASABE* **50**, 885–900.
- Nash J and Sutcliffe J** (1970) River flow forecasting through conceptual models part I – a discussion of principles. *Journal of Hydrology* **10**, 282–290.
- Oleson KW, Dai Y, Bonan G, Bosilovich M, Dickinson R, Dirmeier P, Hoffman F, Houser P, Levis S and Niu GY** (2004) *Technical Description of the Community Land Model (CLM)*. NCAR Technical Note NCAR/TN-461+ STR. Boulder, CO, USA: National Center for Atmospheric Research.

- Omonode RA, Vyn TJ, Smith DR, Hegyemegi P and Gál A** (2007) Soil carbon dioxide and methane fluxes from long-term tillage systems in continuous corn and corn–soybean rotations. *Soil & Tillage Research* **95**, 182–195.
- Pacaldo RS** (2012) *Carbon balances in shrub willow biomass crops along a 19-year chronosequence as affected by continuous production and crop removal (tear-out) treatments* (Traditional thesis). Syracuse, New York, USA: State University of New York.
- Parkin TB and Venterea RT** (2010) Chamber-based trace gas flux measurements. In Follett RF (ed.), *Sampling Protocols*, pp. 1–39. Available at <https://www.ars.usda.gov/ARSUserFiles/np212/Chapter%203.%20GRACEnet%20Trace%20Gas%20Sampling%20Protocols.pdf> (Accessed 12 December 2021).
- Parton WJ, Schimel DS, C.V. C and Ojima DS** (1987) Analysis of factors controlling soil organic matter levels in great plains grasslands. *Soil Science Society of America Journal* **51**, 1173–1179.
- Parton WJ, Hartman M, Ojima D and Schimel D** (1998) DAYCENT and its land surface submodel: description and testing. *Global and Planetary Change* **19**, 35–48.
- Poll C, Marhan S, Back F, Niklaus PA and Kandeler E** (2013) Field-scale manipulation of soil temperature and precipitation change soil CO₂ flux in a temperate agricultural ecosystem. *Agriculture, Ecosystems & Environment* **165**, 88–97.
- Raich J and Schlesinger WH** (1992) The global carbon dioxide flux in soil respiration and its relationship to vegetation and climate. *Tellus B* **44**, 81–99.
- Rawls WJ, Brakensiek DL and Saxton KE** (1982) Estimation of soil water properties. *Transactions of the ASAE* **25**, 1316–1320.
- R Core Team** (2020) *R: A Language and Environment for Statistical Computing*. Vienna, Austria: R Foundation for Statistical Computing. Available at <http://www.R-project.org/>.
- Reilly JM, Jacoby HD and Prinn RG** (2003) *Multi-Gas Contributors to Global Climate Change: Climate Impacts and Mitigation Costs of non-CO₂ Gases*. Arlington, VA, USA: Pew Center on Global Climate Change. Available at <https://www.c2es.org/site/assets/uploads/2003/02/multi-gas-contributors-global-climate-change.pdf>.
- Riveros-Iregui DA, Emanuel RE, Muth DJ, McGlynn BL, Epstein HE, Welsch DL, Pacific VJ and Wraith JM** (2007) Diurnal hysteresis between soil CO₂ and soil temperature is controlled by soil water content. *Geophysical Research Letters* **34**, 17.
- Rochette P and Flanagan LB** (1997) Quantifying rhizosphere respiration in a corn crop under field conditions. *Soil Science Society of America Journal* **61**, 466–474.
- SAS** (2013) *The SAS System for Windows. Release 9.4*. Cary, NC, USA: SAS Institute.
- Schimel JP and Clein JS** (1996) Microbial response to freeze-thaw cycles in tundra and taiga soils. *Soil Biology and Biochemistry* **28**, 1061–1066.
- Soccimarro E, Gualdi S, Bellucci A, Sanna A, Giuseppe Fogli P, Manzini E, Vichi M, Oddo P and Navarra A** (2011) Effects of tropical cyclones on ocean heat transport in a high-resolution coupled general circulation model. *Journal of Climate* **24**, 4368–4384.
- Scott-Denton LE, Rosenstiel TN and Monson RK** (2006) Differential controls by climate and substrate over the heterotrophic and rhizospheric components of soil respiration. *Global Change Biology* **12**, 205–216.
- Sen PK** (1968) On a class of aligned rank order tests in two-way layouts. *The Annals of Mathematical Statistics*, **39**, 1115–1124.
- Sextstone AJ, Revsbech NP, Parkin TB and Tiedje JM** (1985) Direct measurement of oxygen profiles and denitrification rates in soil aggregates. *Soil Science Society of America Journal* **49**, 645–651.
- Singh J, Knapp H and Demissie M** (2004) *Hydrologic Modeling of the Iroquois River Watershed Using HSPF and SWAT*. ISWS CR 2004–08. Champaign, Illinois, USA: Illinois State Water Survey.
- Smith P, Smith J, Powlson D, McGill W, Arah J, Chertov O, Coleman K, Franko U, Frohling S and Jenkinson D** (1997) A comparison of the performance of nine soil organic matter models using datasets from seven long-term experiments. *Geoderma* **81**, 153–225.
- Smith K, Ball T, Conen F, Dobbie K, Massheder J and Rey A** (2003) Exchange of greenhouse gases between soil and atmosphere: interactions of soil physical factors and biological processes. *European Journal of Soil Science* **54**, 779–791.
- Solutions4u** (2021) SigmaPlot has extensive statistical analysis features. Available at <https://www.solutions4u-asia.com/PDT/SYSTAT/SigmaPlot/SPlot-Statistics.html> (Accessed 12 December 2021).
- Subke J-A and Bahn M** (2010) On the temperature sensitivity of soil respiration: can we use the immeasurable to predict the unknown? *Soil Biology and Biochemistry* **42**, 1653–1656.
- Tang J, Baldocchi DD and Xu L** (2005) Tree photosynthesis modulates soil respiration on a diurnal time scale. *Global Change Biology* **11**, 1298–1304.
- Verstraete W and Focht DD** (1977) Biochemical ecology of nitrification and denitrification. *Advances in Microbial Ecology* **1**, 135–214.
- Wang B, Zha T, Jia X, Wu B, Zhang Y and Qin S** (2014) Soil moisture modifies the response of soil respiration to temperature in a desert shrub ecosystem. *Biogeosciences (Online)* **11**, 259–268.
- Watson RT, Zinyowera MC and Moss RH** (1996) *Climate Change 1995: Impacts, Adaptations and Mitigation of Climate Change: Scientific-Technical Analyses. The Second Assessment Report of the Intergovernmental Panel on Climate Change (IPCC)*. Cambridge, UK: Cambridge University Press.
- Winkler JP, Cherry RS and Schlesinger WH** (1996) The Q₁₀ relationship of microbial respiration in a temperate forest soil. *Soil Biology and Biochemistry* **28**, 1067–1072.
- Yukimoto S, Adachi Y and Hosaka M** (2012) A new global climate model of the meteorological research institute: MRI-CGCM3: model description and basic performance (special issue on recent development on climate models and future climate projections). *Journal of the Meteorological Society of Japan* **90**, 23–64.
- Zhang C, Niu D, Hall SJ, Wen H, Li X, Fu H, Wan C and Elser JJ** (2014) Effects of simulated nitrogen deposition on soil respiration components and their temperature sensitivities in a semiarid grassland. *Soil Biology & Biochemistry* **75**, 113–123.
- Zheng P, Wang D, Yu X, Jia G and Zhang Y** (2021) Effects of drought and rainfall events on soil autotrophic respiration and heterotrophic respiration. *Agriculture Ecosystems & Environment* **308**, 107267.
- Zhou X, Wan S and Luo Y** (2007) Source components and interannual variability of soil CO₂ efflux under experimental warming and clipping in a grassland ecosystem. *Global Change Biology* **13**, 761–775.